Physica C 471 (2011) 217–221

Contents lists available at ScienceDirect

Physica C

journal homepage: www.elsevier.com/locate/physc

Magnetization loops and pinning force of Bi-2212 single-crystal whiskers

S. Altin [a], D.M. Gokhfeld [b,*]

[a] Inonu Universitesi, Fen Edebiyat Fakultesi Fizik Bolumu, Superiletkenlik Arastirma Grubu, 44280 Malatya, Turkey
[b] L.V. Kirensky Institute of Physics SB RAS, Akademgorodok 50/38, 660036 Krasnoyarsk, Russia

ARTICLE INFO

Article history:
Received 23 December 2010
Received in revised form 25 January 2011
Accepted 27 January 2011
Available online 2 February 2011

Keywords:
Bi-2212
Whisker
Magnetization loop
Pinning force
Extended critical state model

ABSTRACT

Dependence of magnetization on applied magnetic field for single-crystal Bi-2212 whiskers was measured at different temperatures. Symmetric and asymmetric magnetization loops were successfully described by the extended critical state model (the extended Valkov–Khrustalev model). Pinning force of whiskers was investigated.

1. Introduction

The $Bi_2Sr_2CaCu_2O_y$ (Bi-2212) superconducting whiskers have been discovered by Matsubara [1]. The single-crystalline nature of the whiskers has attracted great attention among the scientists which tried to fabricate the materials in different dimensions by using different preparation methods [2–10]. The fabrication of whiskers owned flexible property without grain boundary and crystal defect is necessary for technological applications [11,12]. In future, it is believed that superconducting single-crystal whiskers will be most used materials in the technological applications such as micro/nano electronic switches, high current applications and Josephson junction based devices.

Flux pinning is one of the important problems in the applications of high-T_c superconductors. Grain boundaries, stacking fault, crystal defects and impurities behave as the primary flux pinning centers in high-T_c superconductors [13–16]. The application temperature has huge importance for high current and high pinning force. At high temperature, thermal energy causes melting of vortex lattice [17–19].

Magnetic properties of high-T_c superconductors are generally revealed with the pinning mechanisms of the flux lines lattice. Relations between the field dependence of critical current density and the magnetization of superconductors are established in the literature. However theoretical calculation of M–H curves at different temperatures remains a nontrivial work. The critical state model describes satisfactory the high field symmetric M–H loops of high-T_c superconductors at low temperatures [20,21]. At higher temperatures, the M–H loops of high-T_c superconductors in high fields become asymmetric with respect to the $M = 0$ axis, so there is serious discrepancies between the theoretical curves and experimental data. The extended critical state model [22] describes asymmetric $M(H)$ dependencies. However some aspects of the extended critical state model, e.g. the surface equilibrium layer, were questionable. We believe that account of pinning force distribution in granules [23] gives the physical background requested for the extended critical state model.

In this study, the magnetization of single-crystal Bi-2212 whiskers has been studied. Experimental details are described in Section 2. Section 3 includes magnetization loops fitting by the extended version of Valkov–Khrustalev model [23] and analyze of pinning properties of the whiskers.

2. Experimental details

Appropriate amounts of reagent grade Bi_2O_3, $SrCO_3$, $CaCO_3$ and CuO were mixed in agate mortar for 2 h to give a nominal composition of $Bi_3Sr_2Ca_2Cu_3O_{10+\delta}$. The mixtures were melted in an α-Al_2O_3 crucibles at 1150 °C for 3 h. Molten material was then quenched between two cold copper plates. Thus, rapidly quenched, pore-free, and approximately 1.5 mm thick amorphous plates were obtained. Whiskers were then grown in a PID controlled tube furnace by heating the glass plates in air. The best whisker growth was obtained at 850 °C for 120 h. Whiskers have sizes ~1 μm × 10 μm × 1 cm.

The whiskers obtained after heat treatment were first examined using Xray powder diffractometer (XRD). The Rigaku RadB system

* Corresponding author. Tel.: +7 391 2494838.
E-mail address: gokhfeld@yandex.ru (D.M. Gokhfeld).

0921-4534/$ - see front matter © 2011 Elsevier B.V. All rights reserved.
doi:10.1016/j.physc.2011.01.006

having CuK_α radiation (λ = 1.5405 Å) with a scan rate of 3°/min between 2θ = 2–60° was used during the XRD measurements. Microstructural and compositional investigations of the whiskers were performed using a LEO EVO-40XVP Scanning Electron Microscope (SEM) with BRUKER Energy Dispersive X-ray Spectroscope (EDX). The magnetic properties of the whiskers were carried out using Cryogenic Q-3398 Vibrating Sample Magnetometer system (VSM) with magnetic fields up to 5 *T* and 7 *T* applied parallel to the main axis of whiskers.

3. Results and discussion

In the XRD pattern of whiskers, Fig. 1, only *c*-axis oriented sharp (00*l*) peaks were observed. The peaks on pattern were indexed as the Bi-2212 phase. This indicates three dimensional regular and perfect atomic arrangements in the whisker. We observed that XRD peaks are relatively wide compared to other studies [24]. In XRD measurement, we pelletized a number of whiskers from same batch and so some whiskers in the pellet have caused to mis-orientation or structural distortion. These effects should be provoked to XRD line broadening. The XRD pattern indicated that the whiskers have tetragonal crystal symmetry and the calculated unit cell parameters were found to be $a = b$ = 5.40 Å and c = 30.59 Å. These results are very close to the previously reported ones for Bi-2212 single-crystal material [25–27].

SEM investigations have revealed that whiskers have very smooth surface morphology and they have not grain boundaries in any direction of growth and no substructure or dislocations. Elemental dot mapping of Bi-2212 whiskers is given in Fig. 2. Surface mapping of whiskers showed homogeneous elemental distributions of Bi, Sr, Ca and Cu and very small amount of Al (0.5%).

The DC magnetization curve versus temperature (*M*–*T*) of the whiskers under 0.01 *T* magnetic fields are shown in Fig. 3. For both the whiskers, a sharp drop in the magnetization was obtained with decreasing temperature, suggesting a good diamagnetic property. The onset temperature of diamagnetic signal, T_c, was found to be 83.2 K.

The experimental data are typical for Bi-2212 single-crystal superconductors and whiskers [3]. We found that measured magnetization loops of the whiskers differ noticeably one from another. Some whiskers fabricated showed a symmetric hysteresis at 10 K but asymmetric with respect to the M = 0 axis at 20 and 40 K. Also a paramagnetic contribution is noticed in these dependencies. The magnetization loops of such typical whisker, denoted whisker 1, are presented on Fig. 4. Other samples have symmetric $M(H)$ hysteresis (M–H) loops at T up to 30 K. Fig. 5 shows the similar $M(H)$ dependencies of the sample denoted whisker 2.

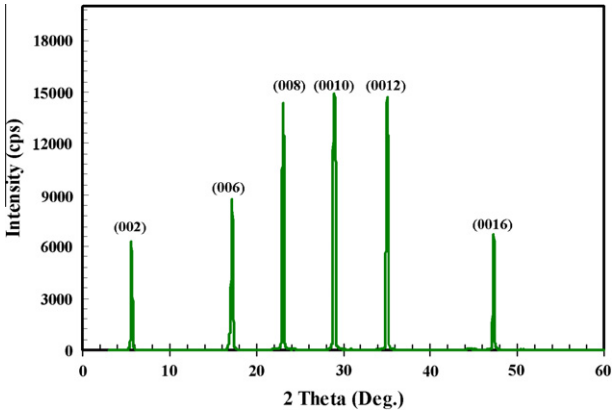

Fig. 1. XRD pattern of whisker fabricated.

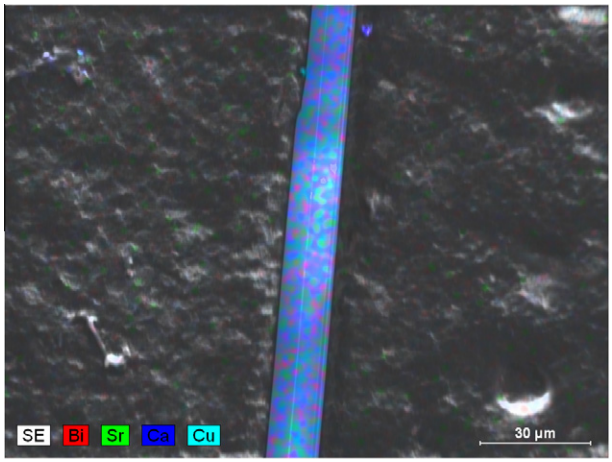

Fig. 2. Elemental dot mapping of whisker fabricated.

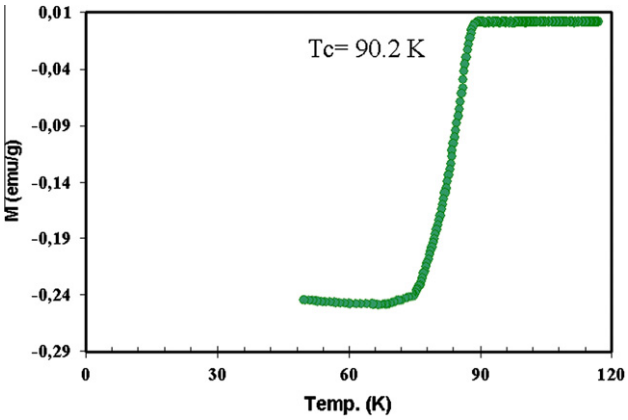

Fig. 3. *M*–*T* measurement of Bi-2212 Whiskers.

All measured magnetization loops of Bi-2212 whiskers were fitted by the extended Valkov–Khrustalev model [23]. The extended Valkov–Khrustalev model is version of the approach [20] modified to be consistent with the extended critical state model [22]. The depth of the equilibrium surface layer, l_s, is accounted in [23]. In the layer from the sample surface to the depth l_s, the pinning force is too weak to hold the vortices unmoved. It is due to the magnetic field distribution in a sample [23]. The parameter l_s is about the London magnetic penetration depth λ and determines the size of a surface layer with equilibrium (reversible) magnetization [22].

There is good agreement between experimental and theoretical *M*–*H* curves at all temperatures (Figs. 4 and 5). The paramagnetic contribution M_P is added empirically to all computed curves (this addition is imperceptible for whisker 2) as $M_P = 0.15[T^{-1}\cdot emu/cm^3]\cdot H$. Some discrepancy observed at small fields may be due to the surface barrier unaccounted and the demagnetizing factor of the sample. We have accepted d = 10 µm for value of the whiskers size in the plane perpendicular *H*. The resulted fitting parameters J_{c0} and l_{s0} for the whiskers 1 and 2 are listed in Table 1. The parameter J_{c0} is the maximal critical current density and l_{s0} is the minimal depth of the equilibrium layer at given *T*. The values of J_{c0} (Table 1) are about 3 times larger than the estimations of J_c from the Bean model. The simple dependence $l_s(H) = l_{s0}\,(1 + H/(0.3H_{irr}))$ is assumed [23]. The $M(H)$ curves were computed with the dependence of the critical current density J_c on the magnetic induction *B* [20]:

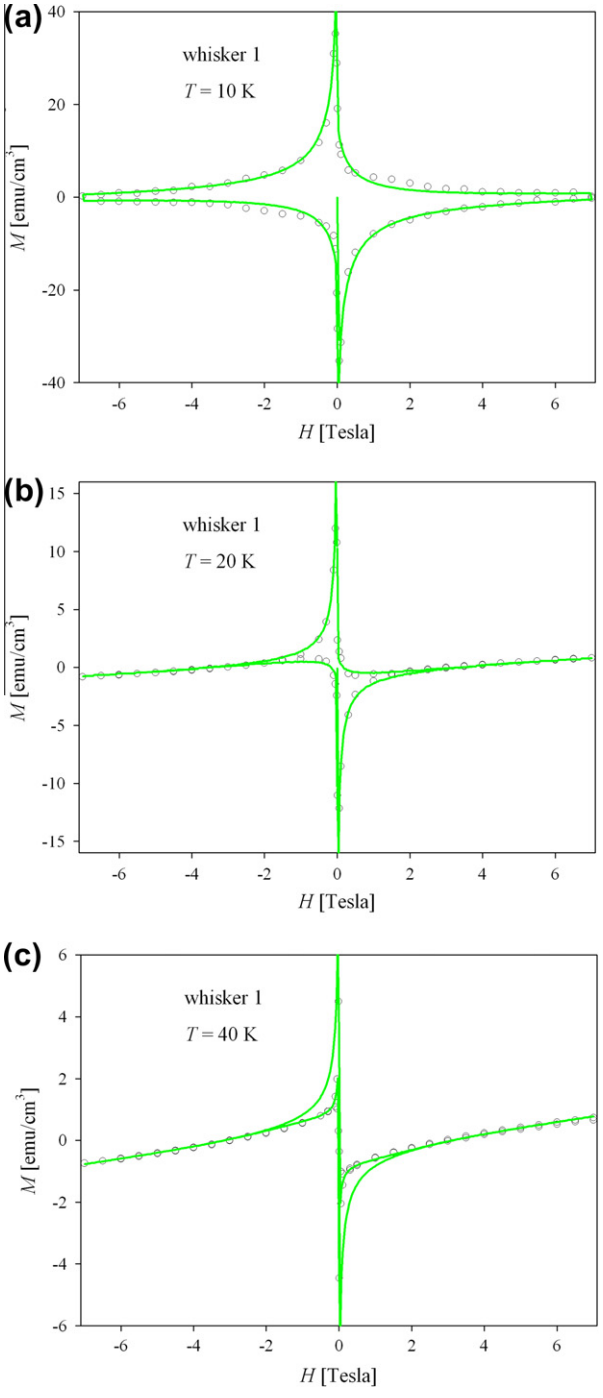

Fig. 4. Experimental (points) and theoretical (lines) M–H curves of Bi-2212 whisker 1 at (a) 10 K, (b) 20 K and (c) 40 K.

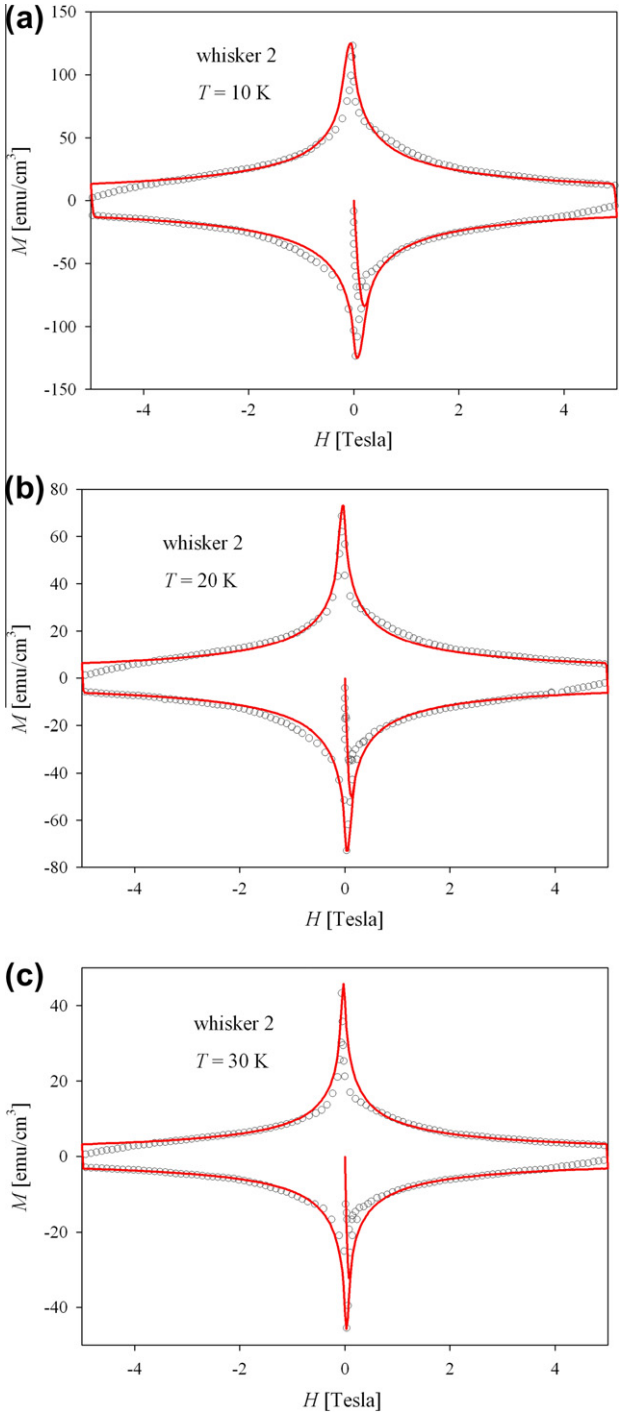

Fig. 5. Experimental (points) and theoretical (lines) M–H curves of Bi-2212 whisker 2 at (a) 10 K, (b) 20 K and (c) 30 K.

$$J_c(B) = \frac{J_{c0}}{\frac{1+QB/B_1}{1+B/B_1} + \left(\frac{B}{B_0}\right)^g}, \quad (1)$$

where B_1 and B_0 are the parameters with the induction measure which determine the characteristic scales. Dimensionless parameters $Q>0$ and $g>0$ determine the decrease rate on these scales. The whiskers magnetization dependencies were fitted with $Q = 5$, $g = 0.75$. The characteristic scales B_1 and B_0 were ~150 and 300 Oe at $T = 4.2$ K and ~10 Oe at 30–40 K. It should be noted that the $J_c(B)$ dependence is not identical a sample averaged $\overline{j_c}(H)$ dependence which can be determined from transport measurements of

Table 1
Fitting parameters of the extended Valkov–Khrustalev model. Maximal critical current density J_c and depth of the equilibrium surface layer l_s. Estimations made for the whiskers size $d = 10$ m km.

T (K)	10	20	30	40
Whisker 1				
J_c 10^6 (A/cm^2)	9	4.5	–	3
$2l_s/d$	0.1	0.18	–	0.3
Whisker 2				
J_c 10^6 (A/cm^2)	41	22	14	–
$2l_s/d$	~0.001–0.01			–

the critical current density in a single-crystal. The expression (1) is determined the local J_c at any point of the sample correspondingly to the distribution of B in the sample. To rule out the sample averaged $\overline{j_c}(H)$ with the extended Valkov–Khrustalev model one should account ratio between the size of the central region with the critical state magnetization [22,23] and the full size of sample. For cylindrical sample it is $\pi(d/2-l_s(H))^2/\pi(d/2)^2$. Then $\overline{j_c}(H=0) = J_{c0}*(1-(2l_{s0}/d)^2)$. The detailed description of $\overline{j_c}(H)$ determination will be given in other work.

The magnetization loop becomes asymmetric when the depth of the layer with equilibrium (reversible) magnetization l_s is comparable with the whiskers size d. When $2l_s/d \geqslant 1$, the $M(H)$ dependence is reversible. The estimated J_{c0} and l_{s0} (Table 1) support that an aggregate pinning in whisker 1 is much weaker than in whisker 2.

The magnetization of the whiskers regularly decreased with increasing magnetic field and temperature. Flux pinning in the $Bi_2Sr_2CaCu_2O_{8+\delta}$ superconductor is influenced by both its crystallographic layered structure (the so-called intrinsic pinning) and the structure of internal defects present in the material [28–30]. At low temperatures, the intrinsic pinning is strong and the flux mostly penetrates a crystal as Josephson vortices. Magnetization caused by the intrinsic pinning became smaller with the increase of temperature. Then the vortex motion starts in the material, which leads to deterioration of the magnetic configuration of fluxes [31–33].

For type II superconductors in the mixed state, J_c depends on the pinning force, F_p, which stabilizes the vortex structure in the presence of a Lorentz force [34]. J_c is defined by $F_p = J_c \times B$ at which the Lorentz force is supported by the pinning structure of the material. F_p is assumed as a function depending on the microstructure and thermodynamic properties of the material. Figs. 6 and 7 shows the magnetic field dependence of F_p of whiskers 1 and 2 at three different temperatures. The Bean model formula was used here to estimate J_c from the loop width. F_p presented a maximum at a certain magnetic field value. This maximum decreased with increasing the temperature. It should be noted that the position of the peak in F_p shifted to higher magnetic fields. At low temperatures, strong pinning forces are very effective whereas in high temperature region (>40 K), the pinning forces are very weak compared to the thermal activation effects [35]. At intermediate temperatures, between 10 and 30 K, different pinning mechanisms have been proposed for the Bi-2212 superconducting system (Fig. 7). According to the scenario proposed by Kadowaki , maximum peak in F_p may be related to the collective pinning of pancake vortices [36]. In the another mechanism, a crossover from 3D flux lines to 2D pancake vortices at high fields and temperatures due to the weak coupling between the superconducting layers in Bi-2212 system can be the reason for this behavior [37–39].

Different values of the pinning force in the samples may be due to diversity of point defects in the whiskers. However there is one more possible explanation of different pinning parameters. The extended Valkov–Khrustalev model [23] predicts strong dependence of the magnetic J_c, determined from the magnetization loop width, on the sample size d. If the relation $2l_s/d$ is much smaller than 1 (the Bean model limit), which works for thick samples, then magnetic J_c is maximal and almost independent of d. When $2l_s(H)/d$ is rising to 1, the magnetic J_c is decreasing till 0 as $\sim(1-(2l_s(H)/d)^2)$. Thus different point defects distribution and size inequality define the different pinning force dependencies of whiskers.

In conclusion, the magnetization loops of Bi-2212 whiskers were measured in high fields at different temperatures. The different type of magnetization loops were observed on the whiskers of one group. The dependencies of pinning force on magnetic field which are estimated from magnetization loops demonstrate different positions of the maximum. The extended Valkov–Khrustalev model was applied to describe the magnetization loops at different temperatures. It is argued that for small samples (with $d \sim \lambda$) the estimated pinning force may be defined not only the point defects but the sample size too.

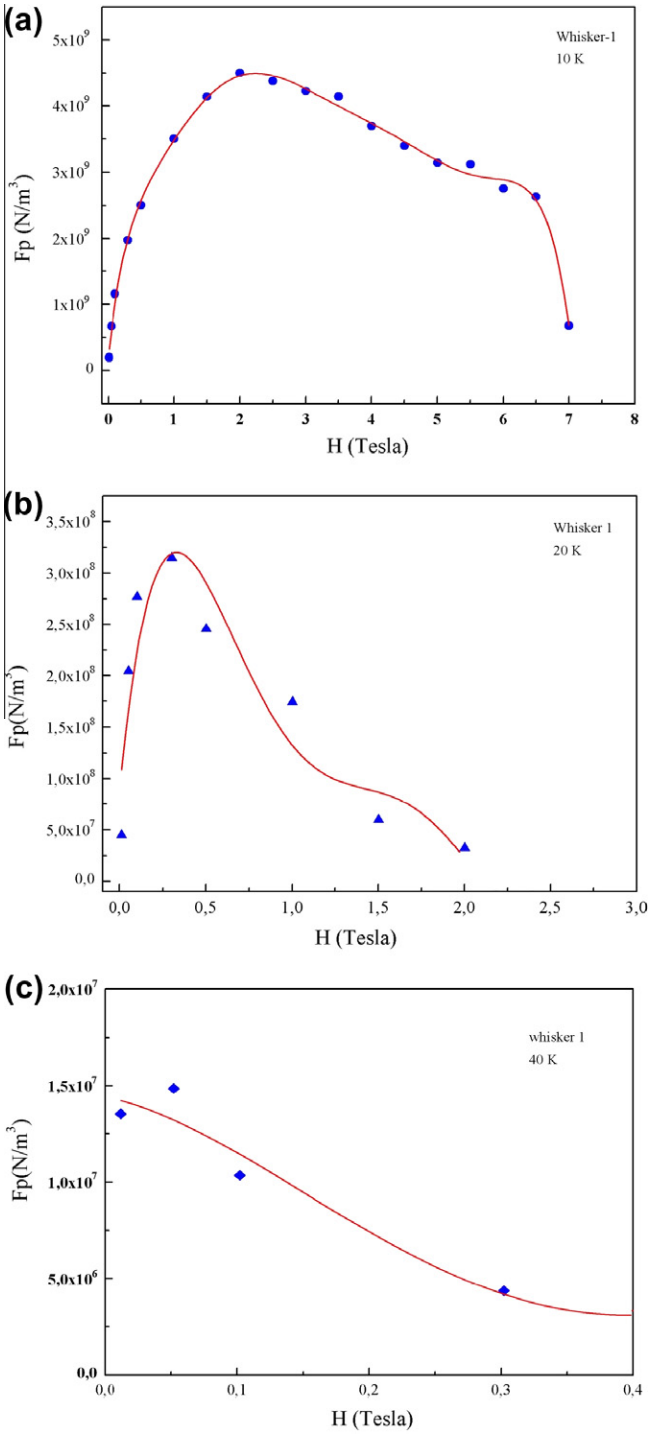

Fig. 6. Pinning force of Bi-2212 whisker 1 at (a) 10 K, (b) 20 K and (c) 40 K.

Acknowledgments

The work is supported by Project No. 7 of RAS Program "Quantum physics of condensed matter", Grant No. 13 of Lavrentyev competition of young researchers of SB RAS and Scientific and

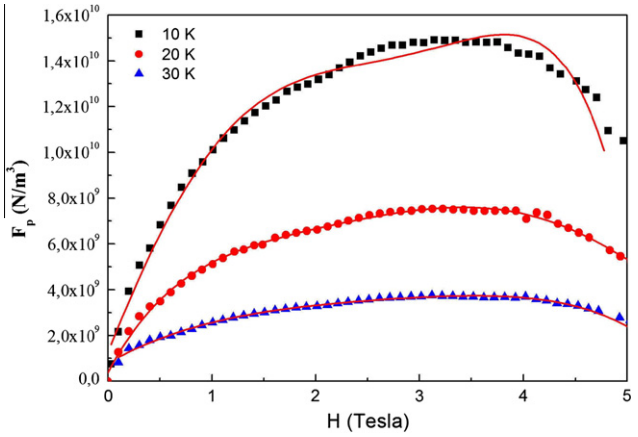

Fig. 7. Pinning force of Bi-2212 whisker 2 at 10 K, 20 K and 30 K.

Technical Research Council of Turkey (TÜBİTAK) under Contract No. TUBITAK-109T747.

References

[1] I. Matsubara, H. Kageyama, H. Tanigawa, T. Ogura, H. Yamashita, T. Kawai, Jpn. J. Appl. Phys. 28 (1989) L1121.
[2] S.-Y. Oh, S.-J. Kim, G.-S. Kim, M. Nagao, T. Hatano, Physica C 445 (2006) 459.
[3] P. Badica, K. Togano, S. Awaji, K. Watanabe, H. Kumakura, Supercond. Sci. Technol. 19 (2006) R81.
[4] M. Tange, M. Yokoshima, Y. Arao, H. Ikeda, R. Yoshizaki, Physica C 426 (2005) 563.
[5] H. Uemoto, M. Mizutani, S. Kishida, T. Yamashita, Physica C 392 (2003) 512.
[6] H. Uemoto, H. Tanaka, T. Hirao, S. Kishida, S.J. Kim, T. Yamashita, Physica C 378 (2002) 303.
[7] S. Kishida, T. Hirao, S.J. Kim, T. Yamashita, Physica C 362 (2001) 195.
[8] I. Matsubara, R. Funahashi, Matt. Res. Bull. 36 (2001) 1639.
[9] I. Matsubara, R. Funuhashi, K. Ueno, H. Ishikawa, J. Cryst. Growth 167 (1996) 570.
[10] T. Kasuga, H. Kimura, Y. Ishigure, Y. Abe, J. Cryst. Growth 144 (1994) 375.
[11] R.L. Jacobsen, T.M. Tritt, A.C. Ehrlich, D.J. Gillespie, Phys. Rev. B 47 (1993) 8312.
[12] I. Matsubara, H. Yamashita, T. Kawai, J. Cryst. Growth 128 (1993) 719.
[13] L. Ammor, A. Ruyter, V.A. Shaidiuk, N.H. Hong, D. Plessis, Phys. Rev. B 81 (2010) 094521.
[14] S. Altin, M.A. Aksan, Y. Balci, M.E. Yakinci, J. Supercond. Novel Magn. 22 (2009) 775.
[15] S. Vinu, P.M. Sarun, R. Shabna, A. Biju, U. Syamaprasad, J. Appl. Phys. 104 (2008) 043905.
[16] E. Giannini, R. Gladyshevskil, N. Clayton, N. Musolino, V. Garnier, A. Piriou, R. Fluekiger, Curr. Appl. Phys. 8 (2008) 115.
[17] P. Spathis, M. Konczykowski, C.J. van der Beek, P. Gierlowski, M. Li, P.H. Kes, Physica C 460 (2007) 1218.
[18] Y.I. Latyshev, V.N. Pavlenko, A.P. Orlov, J. Exp. Theor. Phys. 105 (2007) 235.
[19] K. Hirata, S. Ooi, S. Yu, T. Mochiku, Physica C 445 (2006) 232.
[20] V.V. Val'kov, B.P. Khrustalev, JETP 80 (1995) 680.
[21] D.M. Gokhfeld, D.A. Balaev, S.I. Popkov, K.A. Shaykhutdinov, M.I. Petrov, Physica C 434 (2006) 135.
[22] D.X. Chen, R.W. Cross, A. Sanchez, Cryogenics 33 (1993) 695.
[23] D.M. Gokhfeld, D.A. Balaev, M.I. Petrov, S.I. Popkov, K.A. Shaykhutdinov, V.V. Valkov, J. Appl. Phys. 109 (2011) 033904.
[24] T. Ishigaki, S. Adatch, S. Honda, S. Kishida, H. Tanaka, Physica C 463-465 (2007) 436;
M. Mizutani, H. Uemoto, M. Okabe, S. Kishida, Physica C 392–396 (2003) 508.
[25] K. Inomata, T. Kawae, S.-J. Kim, K. Nakajima, T. Yamashita, M. Nagao, H. Maeda, Physica C 372–376 (2002) 335.
[26] M. Trucatto, G. Rinaudo, C. Manfredotti, A. Agostino, P. Benzi, P. Volpe, C. Paolini, P. Plivero, Supercond. Sci. Technol. 15 (2002) 1304.
[27] S. Altin, M.A. Aksan, M.E. Yakinci, Y. Balci, J. Alloys Compd. 502 (2010) 16.
[28] A. Yurgens, T. Claeson, Physica C 341 (2000) 2277.
[29] P.J. Kung, M.E. Mchenry, M.P. Maley, P.H. Kes, D.E. Laughlin, W.W. Mullins, Physica C 249 (1995) 53.
[30] K. Okamura, M. Kiuchi, E.S. Otabe, T. Yasuda, T. Matsushita, S. Okayasu, Supercond. Sci. Technol. 17 (2004) S20.
[31] O. Ozogul, J. Supercond. Novel Magn. 21 (2008) 223.
[32] S.I. Vedeneev, D.K. Maude, Phys. Rev. B 77 (2008) 064511.
[33] K. Hirata, S. Ooi, T. Mochiku, Physica C 382 (2002) 142.
[34] S. Altin, M.A. Aksan, Y. Balci, M.E. Yakinci, J. Phys. Conf. Ser. 153 (2009) 012004.
[35] J.K. Gregory, M.S. James, S.J. Bending, Phys. Rev. B 64 (2001) 134517.
[36] K. Kadowaki, Sci. Technol. Adv. Mater. 6 (2005) 589.
[37] J. Mirkovic, S. Savelev, E. Sugahara, K. Kadowaki, Physica C 357 (2001) 450.
[38] S.L. Yuan, Z.J. Yang, K. Kadowaki, J.Q. Li, T. Kimura, K. Kishio, Z. Huang, J.L. Chen, B.J. Gao, Appl. Phys. A-Mater. Sci. Process. 59 (1994) 583.
[39] A.I. Rykov, T. Tamegai, Phys. Rev. B 63 (2001) 104519.